



# Polymerization of aniline in the interlayer space of molybdenum trioxide and its electrochemical properties

Yanping Li, Yixian Xiang, Xiaowen Dong, Jiaqiang Xu, Fei Ruan, Qingyi Pan\*

Department of Chemistry, Shanghai University, 99 Shang Da Road, Shanghai 200444, PR China

## ARTICLE INFO

### Article history:

Received 19 January 2009

Received in revised form

25 April 2009

Accepted 2 May 2009

Available online 12 May 2009

### Keywords:

Molybdenum trioxide

Polyaniline

Intercalation

Layered material

Electrochemical property

## ABSTRACT

Molybdenum trioxide/polyaniline ( $\text{MoO}_3/\text{PANI}$ ) composite was prepared first by ion-exchange reaction between aniline (ANI) and dodecylamine (DDA) which was intercalated precursor, and then was formed under the polymerization of ANI within the interlayer space of  $\text{MoO}_3$  at  $120^\circ\text{C}$  for 3 d in air. According to powder X-ray diffraction, scanning electron microscopy, thermogravimetric analysis, infrared spectroscopy and electrochemical testing,  $\text{MoO}_3/\text{PANI}$  composite has layered structure, and its interlayer spacing is 1.127 nm. Moreover, it has high thermal stability with the compound and completes its weight loss at  $751.9^\circ\text{C}$ . Electrochemical investigation shows that  $\text{MoO}_3$  is the major active substance in the  $\text{MoO}_3/\text{PANI}$  electrode, and  $\text{MoO}_3/\text{PANI}$  electrode demonstrates better conductivity and electrochemical activity than pure  $\text{MoO}_3$  electrode, attributed to the promotion of  $\text{Li}^+$  and/or electron transport. In addition, the alternating current impedance proves that if the resistance of  $\text{MoO}_3/\text{PANI}$  electrode reduces apparently, the electrochemical activity will increase correspondingly, the same as the relationship between the ohmic resistance and the electrical conductivity.

© 2009 Elsevier Inc. All rights reserved.

## 1. Introduction

Conductive PANI is considered as the most promising polymer to be used extensively in the future. By nanocompositing with layered compounds, the mechanical properties, stability of interface, thermal stability and processability of PANI will be greatly improved. Besides good conductivity and application perspective in rechargeable cell, this kind of nanocomposites may also have many novel properties, such as photoelectric display, photoelectric transition, thermoelectricity, electromagnetism and electrorheology through the synergic interaction of PANI with layered compounds [1,2].

In recent years, studies on the properties of the intercalated materials have mainly focused on the electrochemical properties. Both the good electron conductivity, proton conductivity and their synergistic reaction have displayed a lot of new properties, enhancing the importance of the studies on how to apply the composite to electrochemistry [3,4]. The intercalated organic–inorganic materials have widely attracted people's attention in these years [5–8]. Among numerous composite of PANI,  $\text{MoO}_3/\text{PANI}$  composite has caused the greatest concerns as it shows many new features in the lithium battery, the gas sensor, etc. [9–14]. However,  $\text{MoO}_3$  does not carry exchangeable ions and its oxidibility is weak. Consequently, it is difficult to intercalate polymers like PANI into the interlayer space of  $\text{MoO}_3$ . Since 1993 when Rabin Bissessur and others initially intercalated PANI into

the interlayer space of  $\text{MoO}_3$  [15], people have been making efforts to find an easy and effective way to prepare the layered  $\text{MoO}_3/\text{PANI}$  composite all along [16–19].

Usually, people primarily reduce  $\text{MoO}_3$  to  $(\text{Li}/\text{Na})_x\text{MoO}_3$  to expand the space between the interlayers, and then fill them with the exchangeable cations in order to intercalate the ANI monomer or the oligomers. However, it is difficult to prepare the precursor of  $(\text{Li}/\text{Na})_x\text{MoO}_3$  as well as to preserve it, and it can only be used in aqueous solution. Thus, we changed the traditional method of preparation by using DDA as intercalation agent to modify  $\text{MoO}_3$  and exchanging it with ANI in the anhydrous acetic acid. Finally, we succeeded in preparing the layered  $\text{MoO}_3/\text{PANI}$  composite with single-layer arrangement of ANI. That is the first step of the in-situ polymerization.

The second step is to use the outside initiators in the polymerization, because of the weak oxidibility of  $\text{MoO}_3$ . In this process, people usually choose the initiators like  $(\text{NH}_4)_2\text{S}_2\text{O}_8$ ,  $\text{FeCl}_3$ , etc. as oxidants. However, in the in-situ polymerization, cations in the oxidant are very likely to replace the ANI and occupy the space between the interlayers [21], even may cause the ANI off the interlayers to form a polymer cover and affect the layered structure. Therefore, on the basis of not breaking the layered structure, we effectively caused the ANI between the interlayers to polymerize and form pure layered  $\text{MoO}_3/\text{PANI}$  composite. The PANI chain in this composite exists in parallel with the interlayer space of  $\text{MoO}_3$ . For the particular conjugated structure of PANI and its highly ordered arrangement between the interlayers, there is an obvious change about electrochemical property of  $\text{MoO}_3$  after it combined with PANI.

\* Corresponding author. Fax: +86 21 62586632.  
E-mail address: [qypan@shu.edu.cn](mailto:qypan@shu.edu.cn) (Q. Pan).

## 2. Experimental

### 2.1. Preparation

All other reagents are of AR grade from Shanghai Chemical Reagent Company.  $\text{MoO}_3$  powder was pre-treated at  $600^\circ\text{C}$  overnight in air prior to use.

The molybdenum oxide/dodecylamine ( $\text{MoO}_3/\text{DDA}$ ) composite as the intermediate product was prepared by the literature method [20], and was then used to prepare molybdenum oxide/aniline ( $\text{MoO}_3/\text{ANI}$ ) [25]. ANI was intercalated by adding excess ANI (10 mL) to a sonicated suspension of 0.5 g  $\text{MoO}_3/\text{DDA}$  composite in anhydrous acetic acid (50 mL), heated at  $70^\circ\text{C}$  for 7 d. After being filtered, washed with absolute ethanol and grilled at  $120^\circ\text{C}$  for 3 d in air, the molybdenum trioxide/polyaniline ( $\text{MoO}_3/\text{PANI}$ ) composite was obtained.

### 2.2. Analysis

The products were characterized by powder X-ray diffraction (D/Max-2550 XRD,  $\text{CuK}\alpha$  radiation). Scanning electron microscopy (SEM) image was obtained with a JEOL JSM-6700F operated at beam energy of 10.0 kV. In addition, infrared spectroscopies were carried out on AVATRA370 IR spectrometer, and thermal analyses (TG-DSC) in  $\text{N}_2$  were performed on thermal analysis system (NETZSCH, STA409PC) at a heating rate of  $10^\circ\text{Cmin}^{-1}$ . The electrochemical property was studied by Solartron brainpower invariable potentiometer.

## 3. Results and discussion

The structure of  $\text{MoO}_3$  consists of vertex-sharing chains of distorted  $\text{MoO}_6$  octahedra [22], which share edges with two similar chains to form layers. The two-dimensional bonded double-octahedra oxide sheets are stacked in a layered arrangement and held together by weak Van der Waals forces.

Fig. 1(a) is the XRD pattern of layered  $\text{MoO}_3$ . From the position of the diffraction peak 0 2 0, we can find out the interlayer spacing ( $d$ ) is 0.692 nm, which is consistent with the reported value [26]. Fig. 1(b)–(d) are, respectively, the XRD patterns of layered  $\text{MoO}_3/\text{DDA}$  composite,  $\text{MoO}_3/\text{ANI}$  and  $\text{MoO}_3/\text{PANI}$ . At the position where the peak 0 1 0 appears, its interlayer spacing ( $d$ ) and the free interlayer spacing ( $\Delta d$ ) compared with the pure  $\text{MoO}_3$  are all included in Table 1. According to Fig. 1(c), after ANI monomer was intercalated, a new strong diffraction peak 0 1 0, whose interlayer spacing is 1.318 nm and free interlayer spacing is 0.626 nm, appeared in a small-angle direction of the XRD pattern of the layered  $\text{MoO}_3/\text{ANI}$  composite compared with the pure layered  $\text{MoO}_3$ . It is similar to the interlayer spacing when layered ANI molecule is vertical to the inorganic interlayer plate [21]. After ANI polymerized via heat treatment in air, its diffraction peak 0 1 0 moves a short distance in the large-angle direction and the interlayer spacing decreases to 1.127 nm. It is notable that after ANI polymerized in the interlayers, the free interlayer spacing becomes 0.435 nm, which is smaller than the diameter of ANI molecule (0.57 nm). So it is impossible to have a monolayer of the PANI to exist vertically with the inorganic interlayer plate [2,14]. The free interlayer spacing is similar to the  $\text{MoS}_2/\text{PANI}$  composite whose intercalated PANI is in parallel with the inorganic layered plate direction in the interlayers [23]. According to this, we infer that the molecules intercalated into the interlayer space of  $\text{MoO}_3$  had turned  $90^\circ$  when triggered by oxygen in air during the polymerization process. That is, the intercalated PANI was parallel with the direction of inorganic layered plate. Fig. 2 is the

**Table 1**  
Interlayer spacing of (a)  $\text{MoO}_3$ , (b)  $\text{MoO}_3/\text{DDA}$ , (c)  $\text{MoO}_3/\text{ANI}$ , and (d)  $\text{MoO}_3/\text{PANI}$ .

Layered composite	$2\theta$ (deg)	$d$ (nm)	$\Delta d$ (nm)
(a) $\text{MoO}_3$	12.78	0.692	
(b) $\text{MoO}_3/\text{DDA}$	2.68	3.086	2.394
(c) $\text{MoO}_3/\text{ANI}$	6.70	1.318	0.626
(d) $\text{MoO}_3/\text{PANI}$	7.84	1.127	0.435

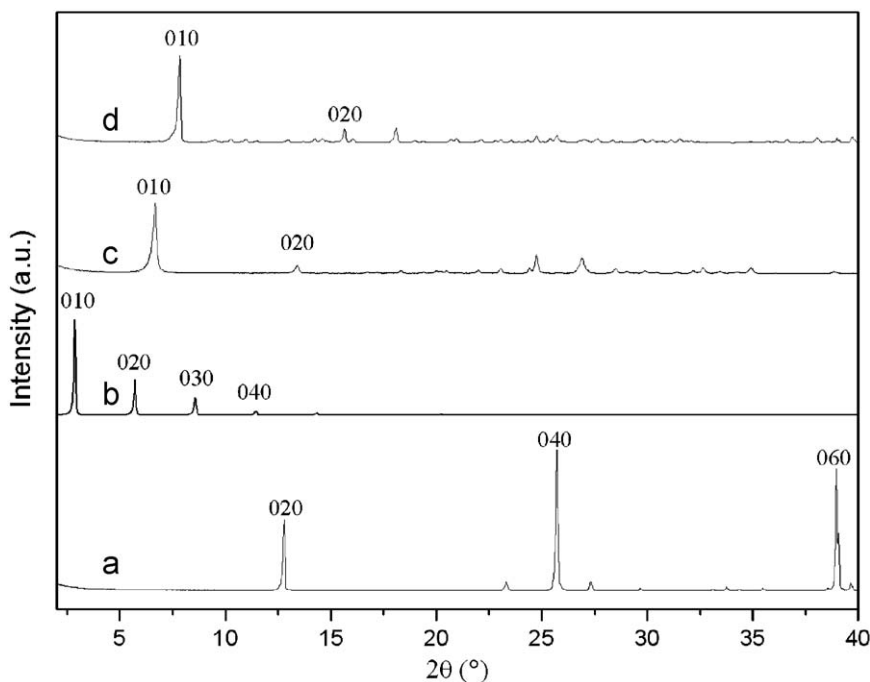


**Fig. 1.** XRD patterns of layered (a)  $\text{MoO}_3$ , (b)  $\text{MoO}_3/\text{DDA}$ , (c)  $\text{MoO}_3/\text{ANI}$ , and (d)  $\text{MoO}_3/\text{PANI}$ .

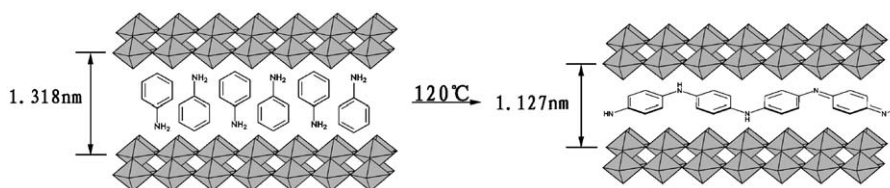


Fig. 2. Schematic presentation of the arrangement of intercalated (a) ANI, and (b) PANI in the interlayer space of  $\text{MoO}_3$ .

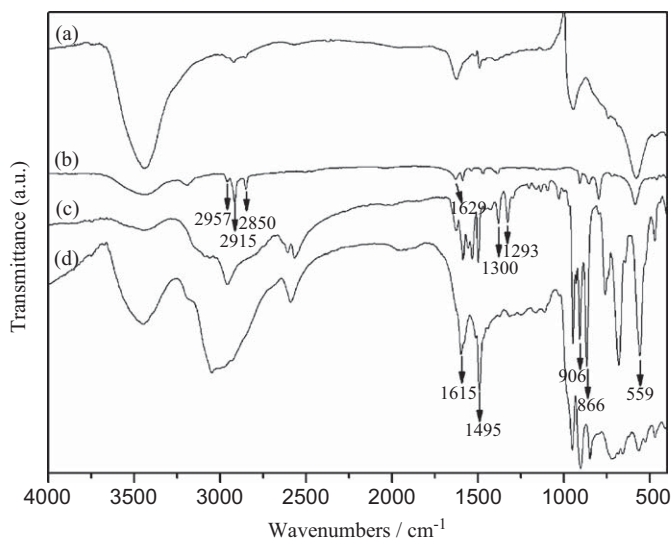


Fig. 3. Infrared spectra of layered (a)  $\text{MoO}_3$ , (b)  $\text{MoO}_3/\text{DDA}$ , (c)  $\text{MoO}_3/\text{ANI}$ , and (d)  $\text{MoO}_3/\text{PANI}$ .

schematic presentation of the arrangement of intercalated (a) ANI and (b) PANI in the interlayer space of  $\text{MoO}_3$ .

Fig. 3(a)–(d) are, respectively, the infrared spectra of layered  $\text{MoO}_3$ ,  $\text{MoO}_3/\text{DDA}$ ,  $\text{MoO}_3/\text{ANI}$  and  $\text{MoO}_3/\text{PANI}$ . Based on the literature value [24], the lattice vibrations of  $\text{MoO}_3$  appear at 581, 868, and  $994\text{ cm}^{-1}$ . Fig. 3(a) indicates the signals of three bands at 586, 865, and  $995\text{ cm}^{-1}$ , which is due to the lattice vibrations of  $\text{MoO}_3$ . As showed in Fig. 3(b), two bands that appeared at 2851 and  $2915\text{ cm}^{-1}$  in the  $\text{MoO}_3/\text{DDA}$  can be attributed to the antisymmetric and symmetric  $\text{CH}_2$  stretching vibrations, respectively. Bands corresponding to NH bending vibration are observed at  $1629\text{ cm}^{-1}$ . After the ANI was intercalated, Fig. 3(c) shows that the lattice vibrations of  $\text{MoO}_3$ , respectively, move to 559, 866, and  $906\text{ cm}^{-1}$ . In addition, two bands at 1496 and  $1615\text{ cm}^{-1}$  in Fig. 3(c) and (d) can be attributed to the stretching vibrations of  $\text{C}=\text{C}$  bond. Bands corresponding to the stretching vibrations of  $\text{C}-\text{N}$  bond are observed at 1293 and  $1300\text{ cm}^{-1}$ . All of these characteristic absorption bands prove that the ANI has polymerized in the interlayer space of  $\text{MoO}_3$ .

Fig. 4 displays the TG–DSC curves of  $\text{MoO}_3/\text{PANI}$  composite under the protection of nitrogen. Corresponding to the literature value [2,10], PANI chain in the whole heat-treatment process is in continuous weight loss, but the weight loss of the composite in literature ranging from 450 to  $550^\circ\text{C}$  is expanded to  $751.9^\circ\text{C}$  here. Thus, the composite has better thermal stability. The TG–DSC curves show that there is a sharp endothermic peak at  $751.9^\circ\text{C}$ , which accords with the main weight loss of PANI. The longer the PANI chain is, the harder it is desorbed by the interlayers. So the composite has an increasing average chain length compared with the  $\text{MoO}_3/\text{PANI}$  composite made by traditional methods. In addition, it is worth noting that: as

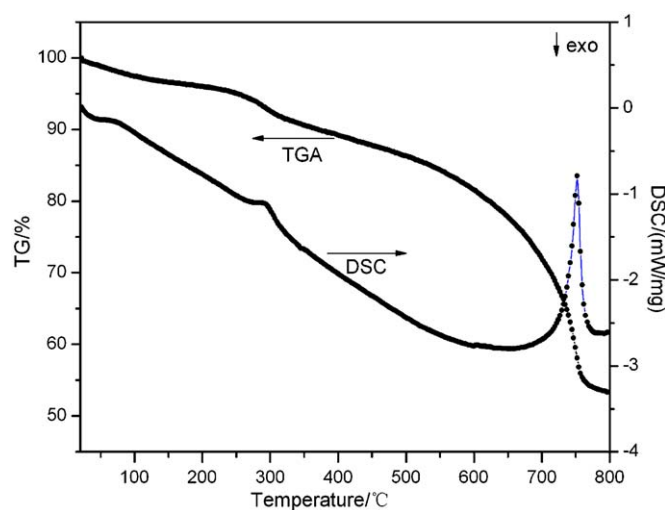


Fig. 4. TG–DSC curves of  $\text{MoO}_3/\text{PANI}$ .

$\text{MoO}_3$  cannot be decomposed under  $800^\circ\text{C}$ , all the weight loss between 20 and  $751.9^\circ\text{C}$  can be regarded as the weight loss of PANI. On such basis, the content of PANI takes 48% of the whole composite, which is 2–3 times more than the composite made by the traditional methods. For the reason that our method uses air as oxidant the products are less polluted by cation oxidation, thus creating a higher purity and a greater polymerization degree of the  $\text{MoO}_3/\text{PANI}$  composite.

Fig. 5 is the cyclic voltammograms of the  $\text{MoO}_3/\text{PANI}$  electrode and the  $\text{MoO}_3$  electrode (containing 15 wt% acetylene black) in  $0.5\text{ mol L}^{-1}\text{ Li}_2\text{SO}_4$  electrolyte. The cyclic scanning ranges from  $-1.0$  to  $1.0\text{ V}$ , and the scan rate is  $5\text{ mV s}^{-1}$ . Because in  $\text{MoO}_3/\text{PANI}$  composite both PANI and  $\text{MoO}_3$  have electrochemical response, their cyclic voltammetry curves are compared and analyzed to have a clearer understanding of the role of PANI in  $\text{MoO}_3/\text{PANI}$  composite.

As is shown in Fig. 5, there are oxidation peaks of both  $\text{MoO}_3/\text{PANI}$  composite and  $\text{MoO}_3$  at the vicinity of  $0.7\text{ V}$ , which have similar shape. But the oxidation peak current of  $\text{MoO}_3/\text{PANI}$  electrode is stronger. According to the literature [2],  $\text{MoO}_3$  and  $\text{Li}^+$  can form certain forms of  $\text{Li}^+$  intercalated composite in aqueous solution, corresponding to oxidation and reduction processes of the cyclic voltammetry curves. As a result, this whole process mainly manifests itself in the intercalation and de-intercalation of  $\text{Li}^+$  in the interlayer space of  $\text{MoO}_3$ . The oxidation peaks of  $\text{MoO}_3/\text{PANI}$  composite and  $\text{MoO}_3$  share similar position at the beginning, that is,  $\text{MoO}_3$  is the main electrochemical active substance in  $\text{MoO}_3/\text{PANI}$  composite electrode. In other words, the electrochemical activity of  $\text{MoO}_3/\text{PANI}$  composite is mainly presented in the intercalation and de-intercalation of  $\text{Li}^+$  in the interlayer space of  $\text{MoO}_3$ . After PANI is intercalated into  $\text{MoO}_3$ , the peak shape of the composite is similar but the area surrounded by has enlarged, which shows the intercalated PANI does not have much effect on

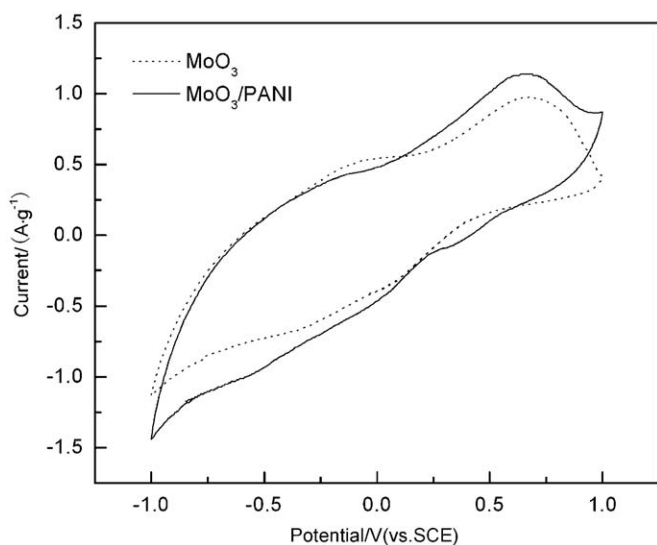


Fig. 5. Cyclic voltammograms of MoO<sub>3</sub>/PANI and pure MoO<sub>3</sub> in 0.5 mol L<sup>-1</sup> Li<sub>2</sub>SO<sub>4</sub> electrolyte. The scan rate is 5 mV s<sup>-1</sup>.

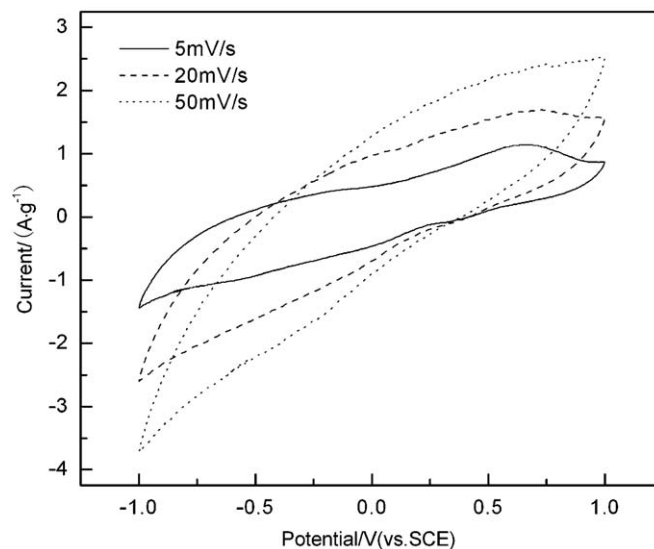


Fig. 6. Cyclic voltammograms at different scan rate of MoO<sub>3</sub>/PANI electrode in 0.5 mol L<sup>-1</sup> Li<sub>2</sub>SO<sub>4</sub> electrolyte.

its redox features, but promotes Li<sup>+</sup> and/or electron transport. The reason may be that the interlayer spacing increased after PANI intercalated into the interlayer space; further, the intercalation and de-intercalation speed of Li<sup>+</sup> in the layered structure of the composite improved.

The whole charge and discharge process of carbon–MoO<sub>3</sub>/PANI battery can be expressed as follows:

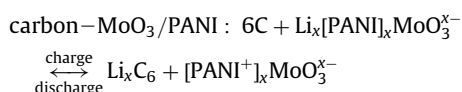
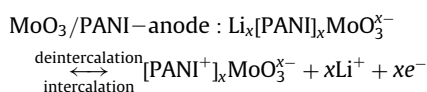
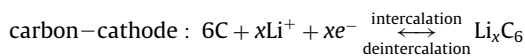


Fig. 6 indicates the cyclic voltammetry curves at different scan rate of MoO<sub>3</sub>/PANI electrode in Li<sub>2</sub>SO<sub>4</sub> 0.5 mol L<sup>-1</sup> electrolyte with the cyclic scanning ranges from -1.0 to 1.0 V. According to Fig. 6, with the increasing of scan rate, the peaks of oxidation and reduction turn to be unnoticeable gradually, and the oxidation peak moves to the forward direction. All above phenomena indicate that it is a quasi-reversible oxidation–reduction reaction.

Fig. 7 shows the alternating current impedance of MoO<sub>3</sub>/PANI electrode. The open circuit potential is -0.04 V, and the range of frequency is from 10<sup>6</sup> to 10<sup>-2</sup> Hz. Fig. 7(b) is the partially enlarged drawing from the section of high frequency in Fig. 7(a). Two spectral lines of alternating current impedance both include a smaller semicircle (in the section of high frequency) and an oblique line with an angle of 45° (in the section of low frequency). It is believed that the semicircle in the section of high frequency is attributed to the charge transfer resistance and the capacitive reactance in the interface between the electrode and the electrolyte. The radius of the semicircles can indicate the magnitude of electrochemical reaction resistance. It is obvious that the semicircle radius of MoO<sub>3</sub>/PANI composite is smaller than that of the pure MoO<sub>3</sub>, suggesting that PANI improves the conductivity of the composite. The oblique line in the section of low frequency corresponds to the Warburg impedance by the diffusion of Li<sup>+</sup> in the solid phase of the electrode. In terms of the

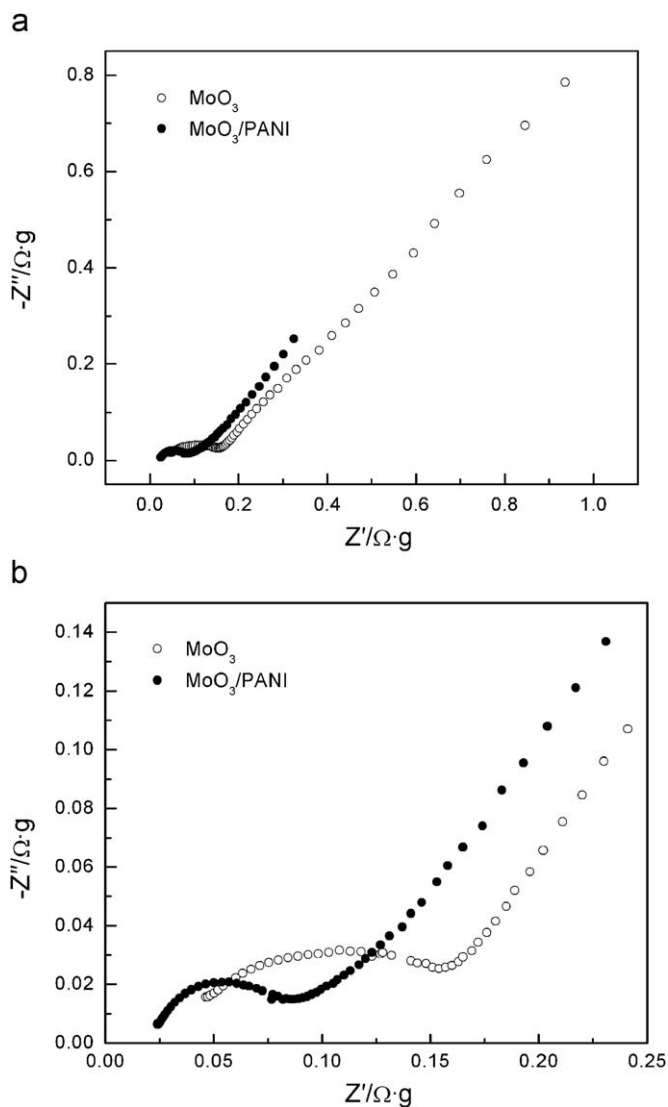


Fig. 7. (a) Alternating current impedance of MoO<sub>3</sub>/PANI and pure MoO<sub>3</sub> electrode. (b) The partial enlarged drawing from the section of high frequency in (a).

value of capacitive reactance arc, the electrochemical reaction resistance of MoO<sub>3</sub>/PANI electrode is lower than that of the pure MoO<sub>3</sub> electrode. What is more, according to Fig. 7(a), the ohmic resistance of MoO<sub>3</sub>/PANI electrode is less than that of pure MoO<sub>3</sub> electrode, which indicates that the electrical conductivity of MoO<sub>3</sub> is increased by intercalating PANI into this composite.

With the increasing of the electrical conductivity of MoO<sub>3</sub>/PANI composite, a reasonable explanation is that PANI exists as the form of electron conjugated extended chain, which is easy for the electron transfer. Besides high electron conductivity, polyamine also can transfer proton and ions. Especially when MoO<sub>3</sub> has a large space structure, the main ions doping/dedoping from PANI will be Li<sup>+</sup>, and further, improves the transfer of Li<sup>+</sup> into the MoO<sub>3</sub> layers and improves the conductivity of the MoO<sub>3</sub>/PANI composite. In addition, former researches about this sort of material mainly focused on anhydrous solution system, while in this study we choose 0.5 mol L<sup>-1</sup> Li<sub>2</sub>SO<sub>4</sub> neutral aqueous solution electrolyte which is easy to prepare and use.

#### 4. Conclusion

Our present study shows that alkylamine is used as the intercalation agent. After intercalating ANI monomer into the interlayer space of MoO<sub>3</sub> in advance, heat treatment at 120 °C for 3 d in air will cause the interlaminar ANI to polymerize, forming layered structure of MoO<sub>3</sub>/PANI composite. We have discarded the traditional method which relies on the precursor of (Li/Na)<sub>x</sub>MoO<sub>3</sub>, initiator and aqueous solution system. Results of X-ray diffraction, SEM and differential thermal analysis indicate that when PANI is intercalated into the interlayer space of MoO<sub>3</sub>, the distance between interlayers will be increased by 0.435 nm, but the composite itself still keeps a layered structure. The interlaminar ANI turns 90° during the polymerization process, existing in parallel with the interlayer plates of MoO<sub>3</sub>. The results of electrochemical test demonstrate that the intercalation of PANI will not change its oxidation and reduction character, but it can promote Li<sup>+</sup> and/or electron to transmit. The electrode reaction of MoO<sub>3</sub>/PANI composite is a quasi-reversible oxidation and reduction reaction. The alternating current impedance proves that if the resistance of MoO<sub>3</sub>/PANI electrode reduces apparently, the electrochemical activity will increase correspondingly, the same as the relationship between the ohmic resistance and the electrical conductivity.

#### Acknowledgments

We appreciate the financial support of Leading Academic Discipline Project of Shanghai Municipal Education Commission (No. J50102). We are also indebted to the Analysis and Research Center at Shanghai University for sample characterization.

#### References

- [1] T.A. Kerr, F. Leroux, L.F. Nazar, *Chem. Mater.* 10 (1998) 2588–2591.
- [2] T.A. Kerr, H. Wu, L.F. Nazar, *Chem. Mater.* 8 (1996) 2005–2015.
- [3] D.J. Maia, S. das Neves, O.L. Alves, M.A. De Paoli, *Electrochim. Acta* 44 (1999) 1945–1952.
- [4] X. Zhang, L.Y. Ji, S.C. Zhang, W.S. Yang, *J. Power Sources* 173 (2007) 1017–1023.
- [5] I. Matsubara, K. Hosono, N. Murayama, W. Shin, N. Izu, *Bull. Chem. Soc. Jpn.* 77 (2004) 1231–1237.
- [6] T. Itoh, I. Matsubara, W. Shin, N. Izu, *Mater. Lett.* 61 (2007) 4031–4034.
- [7] B.S. Wang, X.W. Dong, Q.Y. Pan, Z.X. Cheng, Y.Z. Yang, *J. Solid State Chem.* 180 (2007) 1125–1129.
- [8] J.H. Park, Y.T. Lim, O.O. Park, J.K. Kim, J.-W. Yu, Y.C. Kim, *Adv. Funct. Mater.* 14 (2004) 377–382.
- [9] T. Itoh, I. Matsubara, W. Shin, N. Izu, M. Nishibori, *Sens. Actuators B* 128 (2008) 512–520.
- [10] S. Yoshimoto, F. Ohashi, Y. Ohnishi, T. Nonami, *Synth. Met.* 145 (2004) 265–270.
- [11] C.G. Wu, D.C. DeGroot, H.O. Marcy, J.L. Schindler, C.R. Kannewurf, Y.J. Liu, W. Hirpo, M.G. Kanatzidis, *Chem. Mater.* 8 (1996) 1992–2004.
- [12] J.C. Amicangelo, G.L. Rosenthal, W.R. Leenstra, *Chem. Mater.* 15 (2003) 390–394.
- [13] R. Bissessur, P.K.Y. Liu, W. White, S.F. Scully, *Langmuir* 22 (2006) 1729–1734.
- [14] J.Z. Wang, I. Matsubara, N. Murayama, S. Woosuck, N. Izu, *Thin Solid Films* 514 (2006) 329–333.
- [15] R. Bissessur, D.C. DeGroot, J.L. Schindler, C.R. Kannewurf, M.G. Kanatzidis, *Chem. Commun.* (1993) 687–689.
- [16] X.X. Liu, L.J. Bian, L. Zhang, L.J. Zhang, *J. Solid State Electrochem.* 11 (2007) 1279–1286.
- [17] K. Shao, Y. Ma, Z.H. Chen, X.H. Ji, W.S. Yang, J.N. Yao, *Chem. Lett.* (2002) 322–323.
- [18] O.Y. Posudievsky, S.A. Biskulova, V.D. Pokhodenko, *J. Mater. Chem.* 12 (2002) 1446–1449.
- [19] N. Ballav, M. Biswas, *Mater. Lett.* 60 (2006) 514–517.
- [20] Y. Jing, Q.Y. Pan, Z.X. Cheng, X.W. Dong, Y.X. Xiang, *Mater. Sci. Eng. B* 138 (2007) 55–59.
- [21] K. Hosono, I. Matsubara, N. Murayama, S. Woosuck, N. Izu, *Chem. Mater.* 17 (2005) 349–354.
- [22] H.J. Nam, H. Kim, S.H. Chang, S.G. Kang, S.H. Byeon, *Solid State Ionics* 120 (1999) 189–195.
- [23] M.G. Kanatzidis, R. Bissessur, D.C. DeGroot, J.L. Schindler, C.R. Kannewurf, *Chem. Mater.* 5 (1993) 595–596.
- [24] H. Tagaya, K. Takeshi, K. Ara, J.I. Kadokawa, M. Karasu, K. Chiba, *Mater. Res. Bull.* 30 (1995) 1161–1171.
- [25] Y.X. Xiang, X.W. Dong, Q.Y. Pan, Z.X. Cheng, J.Q. Xu, *Chem. J. Chin. Univ. Chin.* 29 (2008) 1095–1098.
- [26] X.M. Wei, H.C. Zeng, *J. Phys. Chem. B* 107 (2003) 2619–2622.